Progress In Electromagnetics Research Letters, Vol. 53, 65–70, 2015

A Dual-Band Bandpass Filter for 2.4 GHz Bluetooth and 5.2 GHz WLAN Applications

Lakhindar Murmu* **and Sushrut Das**

Abstract—In this paper a dual-band bandpass filter, using stub loaded ring resonator and etched nested C-shape defected ground structure (DGS), is reported. The operating frequencies of the bandpass filter conform to the Bluetooth (2.4 GHz–2.484 GHz) and WLAN (5.15 GHz–5.35 GHz) systems. Due to its applications in WLAN and Bluetooth systems, the filter will be subjected to high EM radiation from the antenna and nearby sources. Therefore, susceptibility study of such filter is very important. The susceptibility study of the filter has been carried out by subjecting the structure to an interference source. Experimental results are presented and analyzed.

1. INTRODUCTION

Microstrip resonators are often used in microwave filters to achieve dual band and multiband characteristics. Among different types of available microstrip resonators, ring resonator has been widely studied due to its high quality (Q) factor and compactness. The ring resonator with the field analysis was first introduced by Wolff and Knoppik [1]. Subsequent studies led to reports of many dual-band ring resonator bandpass filters [2–4]. Dual-band bandpass filter can also be realized using stepped impedance resonator (SIR) [5–9], or by connecting two filter circuits together [10]. However such design suffers from high insertion loss and has the disadvantage of large size. Dual band can also be achieved by using multilayer dielectric [11, 12], but this method is complicated, and the fabrication process is also complex.

Electromagnetic band-gap (EBG) structures are one of the most rapidly advancing topic in the electromagnetic research. They are the artificial periodic structures that prohibit the propagation of electromagnetic waves at microwave or millimeter wave frequencies. Due to its unique stopband and slow-wave effect, planar EBG structures have been widely applied in the design of planar filters for the performance optimization and miniaturization of the circuits [13–15]. Among the different types of planar EBG structures, DGS has been actively studied and applied successfully in the design of various microwave circuits [16, 17]. In [18, 19], DGS was applied to realize the dual-band filters. In [20], split-ring resonators (SRRs) and DGS with constant absolute bandwidth was proposed to generate dual passband. In most planar EBG structures, periodic patches are etched on the ground plane which enhances the inductance of the structure due to the leakage of electromagnetic wave through the etched holes [21]. In [22], the influence of shielding effect of a metallic enclosure on the S-parameters of a shielded EBG microstrip structure was investigated. Although the study of shielding effect was investigated in this paper, the EMC of planar EBG structures remains unexplored.

Since microwave dual band and multiband bandpass filters are an integral part of wireless communication systems (e.g., WLAN/WIMAX/GSM etc.), they are often subjected to microwave radiations. These interfering fields may be either near field type or far field type and can couple

Received 16 April 2015, Accepted 8 May 2015, Scheduled 15 May 2015
* Corresponding author: Lakhindar Murmu (lakhindar.kgec25@gmail.com).
The authors are with the Department of Electronics Engineering, Indian School of Mines, Dhanbad, Jharkhand 826004, India.

with the structure, thereby altering its characteristics. Therefore, in this paper the susceptibility study of the filter has been analyzed by subjecting it to both near field and far field sources.

The main aim of this article is to design a compact dual-band bandpass filter and to study its susceptibility characteristic. A dual-band bandpass filter has been realized using ring resonator with loaded T-shaped stub and nested C-shape DGS. The filter structure has been optimized using parametric analysis, embedded within the electromagnetic (EM) simulator CST microwave studio. The proposed dual-band filter has the advantages of independent control of its resonance frequencies. The proposed dual-band bandpass filter is fabricated and measured to confirm simulation results. Finally, the structure has been subjected to an interfering source for susceptibility testing.

2. RING RESONATOR WITH LOADED STUB

Ring resonators are often used to realize compact microstrip filters at microwave frequencies. As the length of the ring resonator is equal to the multiplication of the mode number and the guided wavelength at resonance frequency, miniaturized structures can be realized using these resonators. In practice, ring resonators are frequency selective and are excited only when the signal frequency is close to the resonance frequency of the rings [23]. The resonance frequency of the ring resonator depends on the total length of the resonator ($2\pi r$), dielectric constant of the substrate, its thickness and trace width. The frequency characteristic of a ring resonator coupled to the microstrip feed line can exhibit either a bandstop or a bandpass response near the resonance frequency depending on the implementation of the ring resonator and the coupling between the feed line and the resonator. As illustrated in Figure 1, the new resonator is comprised of two T-type stubs. A pair of 50-Ω microstrip line feeds the resonator. The dimensions of various design parameters are: $l_1 = 4.8\,\text{mm}$, $l_2 = 6.26\,\text{mm}$, $r_1 = 11.02\,\text{mm}$, $r_2 = 11.72\,\text{mm}$, $w_1 = w_2 = 0.5\,\text{mm}$, $w_3 = 2\,\text{mm}$, $w_4 = 0.5\,\text{mm}$ and $g_0 = 0.2\,\text{mm}$. The simulation has been performed using CST microwave studio. FR-4 substrate with a relative dielectric constant 4.4, thickness $h = 1.59\,\text{mm}$ and loss tangent = 0.02 has been used to design the filter. The simulated frequency response of the filter is shown in Figure 2. The simulated 3-dB fractional bandwidth for the pass band, centered at 2.38 GHz, is found to be 44.09% with a sharpness factor of 72.33 dB/GHz. The insertion loss is less than 0.2 dB, whereas return loss is greater than 19 dB.

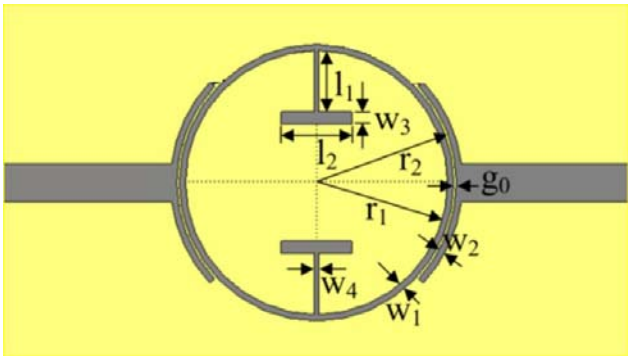

Figure 1. The schematic diagram of bandpass filter.

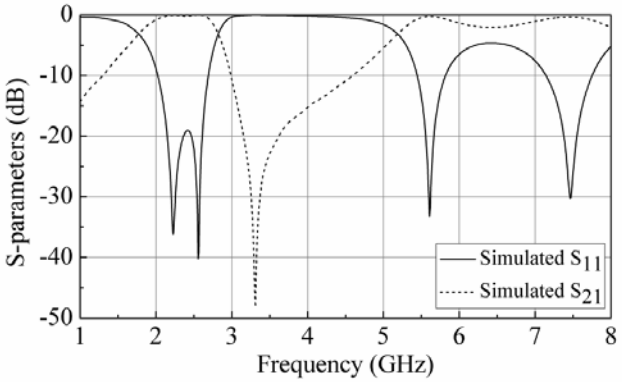

Figure 2. Simulated S-parameters of bandpass filters.

3. DUAL-BAND BANDPASS FILTER USING DGS

DGS can be realized by etching periodic or aperiodic pattern on the ground plane. It can change the effective dielectric constant of the substrate material and disturb the current distribution on the ground plane; hence distributed capacitance and inductance are also changed. The main advantage of DGS is its low pass and band stop character. In this proposed work, nested C-shape DGS is etched on the

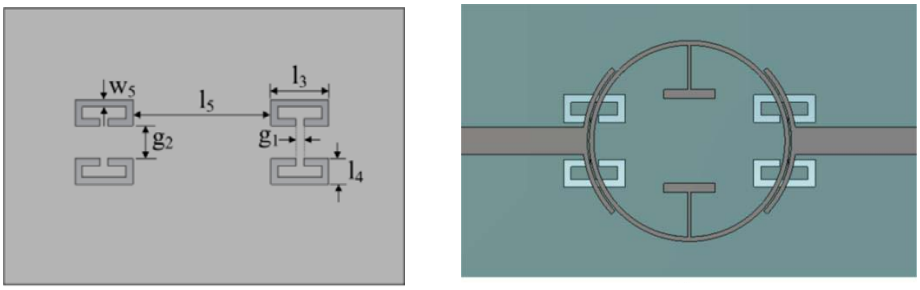

Figure 3. Final dual-band bandpass filter. (a) Nested C-shape DGS structure at ground plane. (b) Transparent view of dual-band bandpass filter.

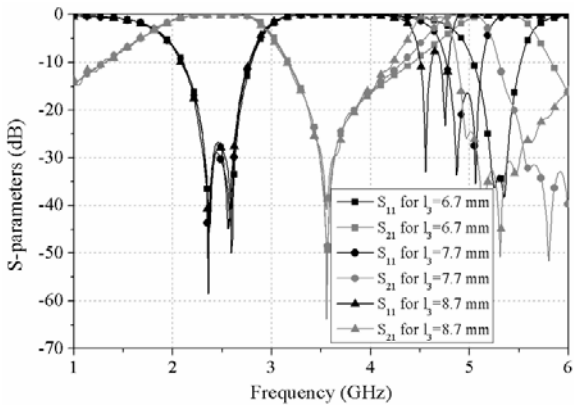

Figure 4. Simulated S-parameters for different DGS length (l_3).

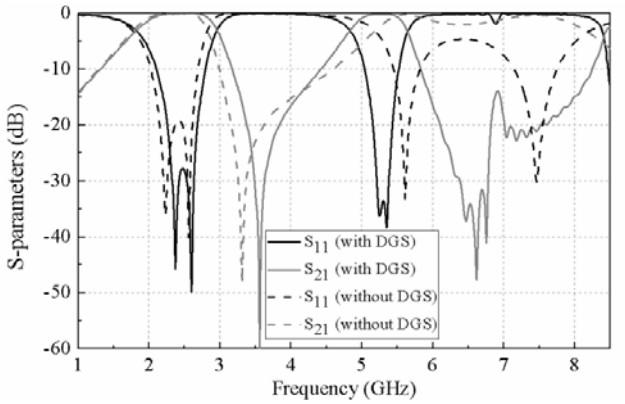

Figure 5. Simulated S-parameters with the effect of DGS.

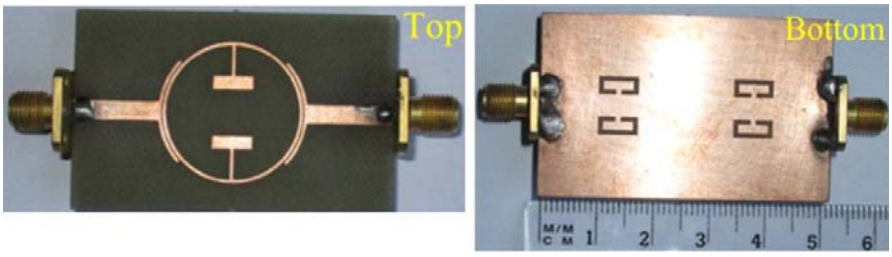

Figure 6. Photograph of the fabricated dual-band bandpass filter (Filter size: 51 mm × 31 mm).

ground plane of the ring resonator bandpass filter to get dual-band response. The final model of the proposed filter is shown in Figure 3.

The simulated filter responses for different DGS lengths (l_3) are shown in Figure 4. It shows that by changing the DGS length, the second passband can be shifted over a wide range, whereas the first passband remains fixed. Thus the second passband can be tuned effectively by adjusting the DGS length l_3. Figure 5 reveals that the filter without DGS has a second pass band with high insertion loss and poor return loss characteristics. However, implementation of DGS structure significantly improves these characteristics and results in a dual band bandpass filter. The pass bands of this filter are centered at 2.47 GHz and 5.29 GHz respectively which covers both Bluetooth 2.4 GHz and WLAN 5.2 GHz. The final dimensions of various design parameters of the dual-band bandpass filter are: $l_1 = 4.8$ mm, $l_2 = 6.26$ mm, $l_3 = 6.7$ mm, $l_4 = 3$ mm, $l_5 = 8.2$ mm, $r_1 = 10.4$ mm, $r_2 = 11.1$ mm, $w_1 = w_2 = 0.5$ mm, $w_3 = 2$ mm, $w_4 = 0.5$ mm, $w_5 =$ mm, $g_0 = 0.2$ mm, $g_1 = 0.9$ mm and $g_2 = 3.82$ mm.

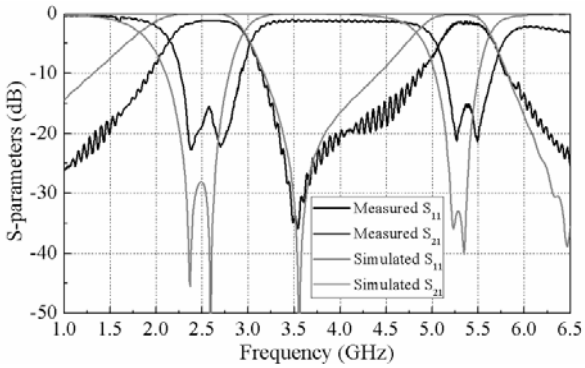

Figure 7. Measured S-parameters result.

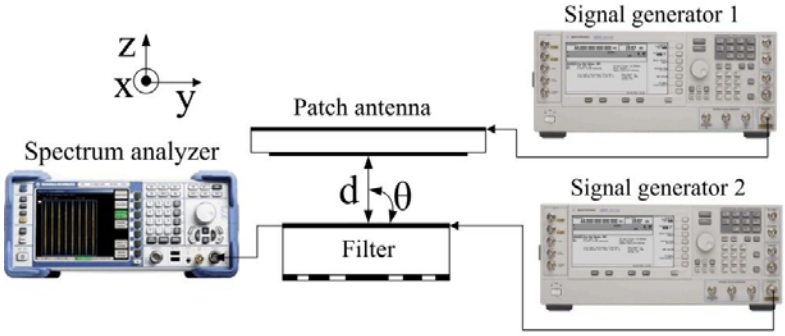

Figure 8. Block diagram of the EMC test setup.

To verify the simulaton, the proposed filter has been fabricated (shown in Figure 6) and its frequency response has been measured. The measurement has been carried out using Agilent E5071B vector network analyzer. Figure 7 shows the simulated and measured results. It reveals that the filter operates at 2.47 GHz with 3-dB fractional bandwidth (FBW) of 45.59% and at 5.29 GHz with 3-dB FBW of 15.33%. So the proposed filter covering both Bluetooth 2.4 GHz, WiMAX 2.5 GHz and WLAN 5.2 GHz bands. The measured insertion losses, including the loss from two SMA connectors, are 1.3 and 1.4 dB at the lower and upper passbands, respectively. The slight frequency deviation observed, is caused by unexpected fabrication tolerance and measurement error.

4. SUSCEPTIBILITY STUDY OF THE FILTER

To do the susceptibility test, the filter was subjected to an interference source. A patch antenna was used to generate the interfering signal. The interference source was placed at a distance d away from the plane under test (PUT) at an angle θ (with respect to the PUT), as shown in Figure 8.

The filter was tested for both near-field (Fresnel region) and far-field (Fraunhofer region) interference sources. Relative power (P_r) is used as a parameter to evaluate the susceptibility characteristics of the filter. The relative power is defined as a ratio between the measured power of the signal when the filter is exposed to interference ($P_{\max}$) and that of the signal when there is no interference ($P_{\min}$) and can be expressed as

$$P_r = \frac{P_{\max}}{P_{\min}} \tag{1}$$

During measurement the filter was excited at port 1 with a signal of frequency $f_c = 2.48$ GHz and power $P_c = -30$ dBm. In order to obtain a strong interference the frequency of the interfering signal is also tuned at 2.48 GHz. The powers transmitted through the filter are recorded at the output of the device

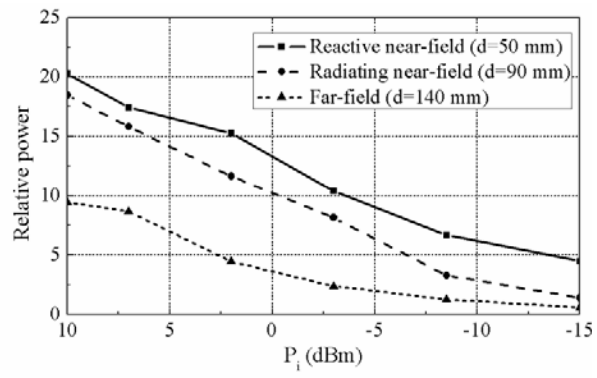

Figure 9. Measured relative power at the output of the filter when the power of the interference source, P_i, is varied from 10 dBm to -15 dBm ($P_c = -50$ dBm).

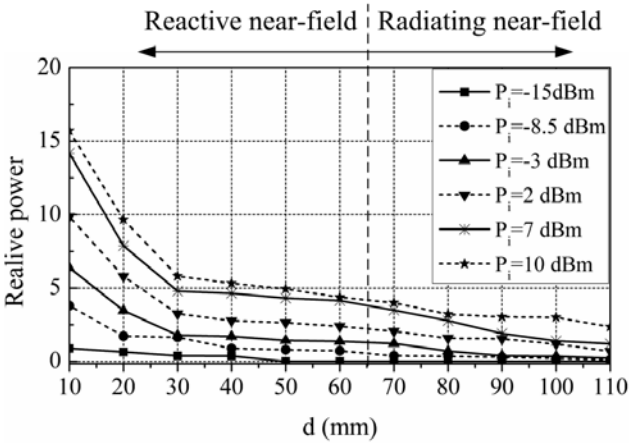

Figure 10. The relative power of a signal at the output of the filter when the distance, d, is varied from near-field to far-field region ($P_c = -30$ dBm).

when the power level of the interference source, P_i is varied from 10 dBm to -15 dBm. The relative powers are plotted against P_i in Figure 9. Figure 9 reveals that P_r decrease gradually as the power level of the interference source decreases, which is expected since the power level of the interference source has a linear relationship with the logarithm of the noise level. Figure 10, plots relative power when the interference source is moved towards the filter. From Figure 10 it is clear that P_r decreases as d increases. This is because the strength of the E-field of the interference source decreases as d increases. The rate of decrease in P_r is high when d increases from 10 mm to 30 mm. P_r becomes relatively small when $d > 70$ mm. The structure is less susceptible to the interference when it is placed more than 110 mm away from the interference source.

Figure 10 reveals that when the incident power is 15 dBm higher than the power of the signal within the filter, the relative power lies below 0.56, even when the source is kept only 10 mm away from the filter. In practice this incident power is very high compared to its practical value as the filter will be subjected only to the radiation from the antenna connected with the system. Since the signal power within the filter is only -30 dBm, the incident power will be much less than -30 dBm due to the presence of path loss, antenna loss and the system losses. Thus the relative power will be much lower than 0.56, which indicate that the filter will work satisfactorily in the presence of interference from the Bluetooth/WLAN antenna.

5. CONCLUSION

In this proposed work, a dual-band bandpass filter has been realized using stub loaded microstrip ring resonator and nested C-shaped DGS. The nested C-shaped DGS have been employed to tune the second passband of the filter. Both the simulated and measured frequency responses are presented, with good agreement between them. Finally, susceptibility test of the structure has been carried out, and the experimental results have been presented and analyzed. The analysis of the experimental data indicates that the system will work satisfactorily in the presence of interference.

REFERENCES

1. Wolff, I. and N. Knoppik, "Microstrip ring resonator and dispersion measurements on microstrip lines," *Electron. Lett.*, Vol. 7, 779–781, 1971.
2. Mondal, P. and M. K. Mandal, "Design of dual-band bandpass filters using stub-loaded open-loop resonators," *IEEE Trans. on Microw. Theory and Tech.*, Vol. 56, No. 1, 150–155, 2008.

3. Chen, F. C., Z. H. Chu, and Q. X. Tu, "Design of compact dual-band bandpass filter using short stub loaded resonator," *Microwave Opt. Technol. Lett.*, Vol. 51, No. 4, 959–963, 2009.
4. Wu, X.-H., Q.-X. Chu, and X.-K. Tian, "Dual-band bandpass filter using novel side-stub-loaded resonator," *Microwave Opt. Technol. Lett.*, Vol. 54, No. 2, 362–364, 2012.
5. Chin, K.-S. and C.-K. Lung, "Miniaturized microstrip dual-band bandstop filters using tri-section stepped-impedance resonators," *Progress In Electromagnetics Research C*, Vol. 10, 37–48, 2009.
6. Chiou, Y.-C., "Transmission zero design graph for dual-mode dual-band filter with periodic stepped-impedance ring resonator," *Progress In Electromagnetics Research*, Vol. 108, 23–36, 2010.
7. You, B., L. Chen, Y. Liang, et al., "A high-selectivity tunable dual-band bandpass filter using stub-loaded stepped-impedance resonators," *IEEE Microw. Wirel. Compon. Lett.*, Vol. 24, No. 11, 736–738, 2014.
8. Chen, C.-F., S.-F. Chang, B.-H. Tseng, and J.-H. Weng, "Compact dual-band stepped-impedance resonator filter with separate coupling paths," *Electronics Letters*, Vol. 50, No. 21, 1551–1552, 2014.
9. Zhang, R. and L. Zhu, "Design of a compact dual-band bandpass filter using coupled stepped-impedance resonators," *IEEE Microw. Wirel. Compon. Lett.*, Vol. 24, No. 3, 155–157, 2014.
10. Miyake, H., S. Kitazawa, and T. Ishizaki, "A miniaturized monolithic dual band filter using ceramic lamination technique for dual mode portable telephones," *IEEE MTT-S Int. Microw. Symp. Dig.*, Vol. 2, 789–792, 1997.
11. Watanbe, T., K. Furutani, and N. Nakajima, "Antenna switch duplexer for dual-band phone (GSM/DCS) using LTCC multilayer technology," *IEEE MTT-S Int. Microw. Symp. Dig.*, Vol. 1, 215–218, 1999.
12. Wang, K., L. Zhu, S.-W. Wong, et al., "Balanced dual-band BPF with intrinsic common-mode suppression on double-layer substrate," *Electron. Lett.*, Vol. 51, No. 9, 705–707, 2015.
13. Garcia-Garcia, J., J. Bonache, and F. Martin, "Application of electromagnetic bandgap to the design of ultra-wide bandpass filters with good out-of-band performance," *IEEE Trans. on Microw. Theory and Tech.*, Vol. 54, 4136–4140, 2006.
14. Yang, F., K. Ma, Y. Qian, and T. Itoh, "A uniplanar compact photonic-bandgap (UC-PBG) structure and its applications for microwave circuit," *IEEE Trans. on Microw. Theory and Tech.*, Vol. 47, No. 8, 1509–1514, 1999.
15. Radonić, V. and V. C. Bengin, "Control of inter-resonator coupling using defected ground structure lattice," *Electron. Lett.*, Vol. 51, No. 5, 399–401, 2015.
16. Ahn, D., J. Park, C. Kim, J. Kim, Y. Qian, and T. Itoh, "A design of the low-pass filter using a novel microstrip defected ground structure," *IEEE Trans. on Microw. Theory and Tech.*, Vol. 49, No. 1, 86–93, 2001.
17. Chaudhary, G., H. Choi, Y. Jeong, et al., "Design of dual-band bandpass filter using DGS with controllable second passband," *IEEE Microw. Wirel. Compon. Lett.*, Vol. 21, No. 11, 589–591, 2011.
18. Song, K., F. Zhang, and Y. Fan, "Miniaturized dual-band bandpass filter with good frequency selectivity using SIR and DGS," *AEU — International Journal of Electronics and Communications*, Vol. 68, No. 5, 384–387, 2014.
19. Jin, X., Z.-H. Zhang, L. Wang, and B.-R. Guan, "Compact dual-band bandpass filter using single meander multimode DGS resonator," *Electron. Lett.*, Vol. 49, No. 17, 1083–1084, 2013.
20. Su, T., L.-J. Zhang, S.-J. Wang, Z.-P. Li, and Y.-L. Zhang, "Design of dual-band bandpass filter with constant absolute bandwidth," *Microwave Opt. Technol. Lett.*, Vol. 56, No. 3, 715–718, 2014.
21. Huang, S. Y. and Y. H. Lee, "Susceptibility of an electromagnetic bandgap filter," *IEEE Transactions on Electromagnetic Compatibility*, Vol. 52, No. 3, 599–603, 2010.
22. Du, Z., K. Gong, J. S. Fu, B. Gao, and Z. Feng, "Influence of a metallic enclosure on the *S*-parameters of microstrip photonic bandgap structures," *IEEE Transactions on Electromagnetic Compatibility*, Vol. 44, No. 2, 324–328, 2002.
23. Chang, K. and L. H. Hsieh, *Microwave Ring Circuits and Related Structures*, 2nd edition, Wiley-Interscience, Hoboken, NJ, 2004.